
Constraining Implicit Space with MDL: Regularity Normalization as Unsupervised Attention

Baihan Lin

Columbia University
baihan.lin@columbia.edu

Abstract

Inspired by the adaptation phenomenon of neuronal firing, we propose the regularity normalization (RN) as an unsupervised attention mechanism (UAM) which computes the statistical regularity in the implicit space of neural networks under the Minimum Description Length (MDL) principle. Treating the neural network optimization process as a partially observable model selection problem, UAM constrained the implicit space by a normalization factor, the universal code length. We compute this universal code incrementally across neural network layers and demonstrated the flexibility to include data priors such as top-down attention and other oracle information. Empirically, our approach outperforms existing normalization methods in tackling limited, imbalanced and non-stationary input distribution in computer vision and reinforcement learning tasks. Lastly, UAM tracks dependency and critical learning stages across layers and recurrent time steps of deep networks.¹

1 Introduction

The Minimum Description Length (MDL) principle asserts that the best model given some data is the one that minimizing the combined cost of describing the model and describing the misfit between the model and data [17] with a goal to maximize regularity extraction for optimal data compression, prediction and communication [6]. Most unsupervised learning algorithms can be understood using the MDL principle [18], treating the neural network (NN) as a system communicating the input to a receiver.

¹The code to reproduce the results can be accessed at: <https://github.com/doerlbh/UnsupervisedAttentionMechanism>

If we consider the neural network training as the optimization process of a communication system, each input at each layers of the system can be described as a point in a low-dimensional continuous constraint space [21]. If we consider the neural networks as population codes, the constraint space can be subdivided into the input-vector space, the hidden-vector space, and the *implicit space*, which represents the underlying dimensions of variability in the other two spaces, i.e., a reduced representation of the constraint space. For instance, if we are given a image of an object, the rotated or scaled version of the same image still refers to the same objects, then each instance of the object can be represented by a code assigned position on a 2D implicit space with one dimension as orientation and the other as size of the shape [21]. The relevant information about the implicit space can be constrained to ensure a minimized description length of the networks.

In this paper, we adopt a similar definition of implicit space as in [21], but extend it beyond unsupervised learning, into a generic neural network optimization problem in both supervised and unsupervised setting. In addition, we consider the formulation and computation of description length differently. Instead of considering neural networks as population codes, we formulate each layer of neural networks during training a state of module selection. In our setup, the description length is computed not in the scale of the entire neural networks, but by the unit of each layer of the network. In addition, the optimization objective is not to minimize the description length, but instead, to take into account the minimum description length as part of the normalization procedure to reparameterize the activation of each neurons in each layer. The computation of the description length (or model cost as in [21]) aims to minimize it, while we directly compute the minimum description length in each layer not to minimize anything, but to reassign the weights based on statistical regularities. Finally, we compute the description length by an optimal universal code obtained by the batch input distribution in an online incremental fashion. This model description

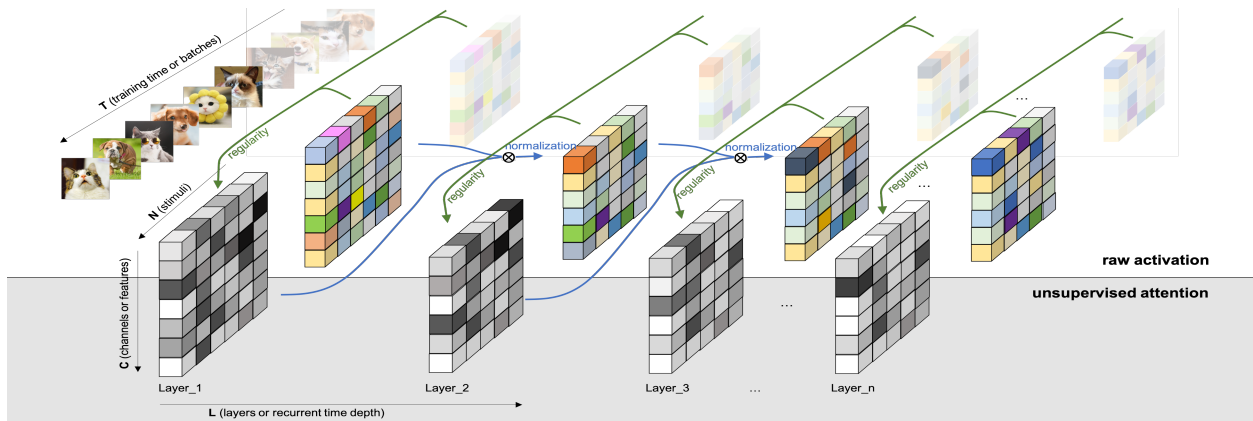


Figure 1: **Unsupervised attention mechanism** is a regularity-based normalization computed sequentially across layers.

serves both as a normalization factor to speed up training and as a useful lens to analyze the information propagation in neural networks. As this approach offers internal regularization across layers to emphasize the gradients of a subset of activating units, we call this framework *Unsupervised Attention Mechanism* (UAM, see Figure 1).

We begin our presentation in section 2, with a short overview of related works in normalization and MDL in neural networks. Section 4 formulated the neural network training process as a layer-specific model selection problem. We then introduce the unsupervised attention mechanism, its standard formulation (regularity normalization, or RN), its implementation, and the incremental tricks for batch computation. We also present several variants of RN by incorporating batch and layer normalizations, termed regularity batch normalization (RBN) and regularity layer normalization (RLN), as well as including the data prior as top-down attention during training, termed saliency normalization (SN). Section 6 analyzed the unsupervised attention mechanism during learning process across neural network layers and recurrent time steps. In section 7, we present the empirical results on the imbalanced MNIST dataset and reinforcement learning games to demonstrate that our approach is advantageous over existing normalization methods in different imbalanced scenarios. In the last section, we conclude our methods and point out several future work directions as the next step of this research.

Our main contribution is two-fold: (1) From the engineering perspective, the work offers a performance improvement of numerical regularization in a imbalanced input data distribution; (2) More importantly, from the analytical perspective, we consider the proposed method a novel way of analyzing and understanding the deep networks during training, learning and failing, beyond its empirical advantages on the non-stationary task setting in the result section. The main point is not simply about beating the

state-of-the-art normalization method with another normalization, but more to offer a new perspective where people can gain insights of the deep network in action – through the lens of model complexity characterized by this normalization factor the model computes along the way. On the subsidiary numerical advantage of our normalization method, the results supported that traditional methods along with our approach can be much stronger than any method by itself, as the regularization priors they each impose are in different dimensions and subspaces.

2 Related work

2.1 Neuroscience inspirations

In biological brains of primates, high-level brain areas are known to send top-down feedback connections to lower-level areas to encourage the selection of the most relevant information in the current input given the current task [4], similar to the communication system above. This type of modulation is performed by collecting statistical regularity in a hierarchical encoding process between these brain areas. One feature of the neural coding during the hierarchical processing is the adaptation: in vision neuroscience, vertical orientation reduce their firing rates to that orientation after adaptation [2], while the cell responses to other orientations may increase [5]. These behaviors contradict to the Bayesian assumption that the more probable the input, the larger firing rate should be, but instead, well match the information theoretical point-of-view that the most relevant information (saliency), which depends on the statistical regularity, have higher “information”, just as the firing of the neurons. As [16] hypothesized that the firing rate represent the code length instead of the probability, similarly, the more regular the input features are (such as after adaption), the lower it should yield the activation, thus a shorter code length of the model (a neuron or a neuronal population).

2.2 Normalization methods in neural networks

Batch normalization (BN) performs global normalization along the batch dimension such that for each neuron in a layer, the activation over all the mini-batch training cases follows standard normal distribution, reducing the internal covariate shift [8]. Similarly, layer normalization (LN) performs global normalization over all the neurons in a layer, and have shown effective stabilizing effect in the hidden state dynamics in recurrent networks [1]. Weight normalization (WN) applied normalization over the incoming weights, offering computational advantages for reinforcement learning and generative modeling [20]. Like BN and LN, we apply the normalization on the activation of the neurons, but as an element-wise reparameterization (over both the layer and batch dimension). In section 5.2, we also proposed the variant methods based on our approach with batch-wise and layer-wise reparameterization, the regularity batch normalization (RBN) and regularity layer normalization (RLN).

2.3 Description length in neural networks

[7] first introduced the description length to quantify neural network simplicity and develop an optimization method to minimize the amount of information required to communicate the weights of the neural network. [21] considered the neural networks as population codes and used MDL to develop highly redundant population code. They showed that by assuming the hidden units reside in low-dimensional implicit spaces, optimization process can be applied to minimize the model cost under MDL principle. Our proposed method adopt a similar definition of implicit space, but consider the implicit space as data-dependent encoding statistical regularities. Unlike [21] and [7], we consider the description length as a indicator of the data input and assume that the implicit space is constrained when we normalize the activation of each neurons given its statistical regularity. Unlike the implicit approach to compute model cost, we directly compute the minimum description length with optimal universal code obtained in an incremental style.

3 Background

3.1 Minimum Description Length

Given a model class Θ consisting of a finite number of models parameterized by the parameter set θ . Given a data sample x , each model in the model class describes a probability $P(x|\theta)$ with the code length computed as $-\log P(x|\theta)$. The minimum code length given any arbitrary θ would be given by $L(x|\hat{\theta}(x)) = -\log P(x|\hat{\theta}(x))$ with model $\hat{\theta}(x)$ which compresses data sample x most

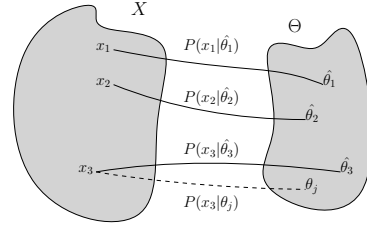


Figure 2: **Normalized maximal likelihood.** In this illustration, data sample x_i are drawn from the entire data distribution X and model $\hat{\theta}_i$ is the optimal model that describes data x_i with the shortest code length. θ_j is an arbitrary model that is not $\hat{\theta}_3$, so $P(x_3|\theta_j)$ is not considered when computing optimal universal code according to NML formulation.

efficiently and offers maximum likelihood $P(x|\hat{\theta}(x))$ [6].

However, the compressibility of the model, computed as the minimum code length, can be unattainable for multiple non-i.i.d. data samples as individual inputs, as the probability distributions of most efficiently representing a certain data sample x given a certain model class can vary from sample to sample. The solution relies on the existence of a universal code, $\bar{P}(x)$ defined for a model class Θ , such that for any data sample x , the shortest code for x is always $L(x|\hat{\theta}(x))$, as shown in [19].

3.2 Normalized Maximum Likelihood

To select for a proper optimal universal code, a cautious approach would be to assume a worst-case scenario in order to make “safe” inferences about the unknown world. Formally, the worst-case expected regret is given by $R(p||\Theta) = \max_q E_q[\ln \frac{f(x|\hat{\theta}_x)}{p(x)}]$, where the “worst” distribution $q(\cdot)$ is allowed to be any probability distribution. Without referencing the unknown truth, [19] formulated finding the optimal universal distribution as a mini-max problem of computing $p^* = \arg \min_p \max_q E_q[\ln \frac{f(x|\hat{\theta}_x)}{p(x)}]$, the coding scheme that minimizes the worst-case expected regret. Among the optimal universal code, the normalized maximum likelihood (NML) probability minimizes the worst-case regret and avoids assigning an arbitrary distribution to Θ . The minimax optimal solution is given by [15]:

$$P_{NML}(x) = \frac{P(x|\hat{\theta}(x))}{\sum_{x'} P(x'|\hat{\theta}(x'))} \quad (1)$$

where the summation is over the entire data sample space. Figure 2 describes the optimization problem of finding optimal model $P(x_i|\hat{\theta}_i)$ given data sample x_i among model class Θ . The models in the class, $P(x|\theta)$, are parameter-

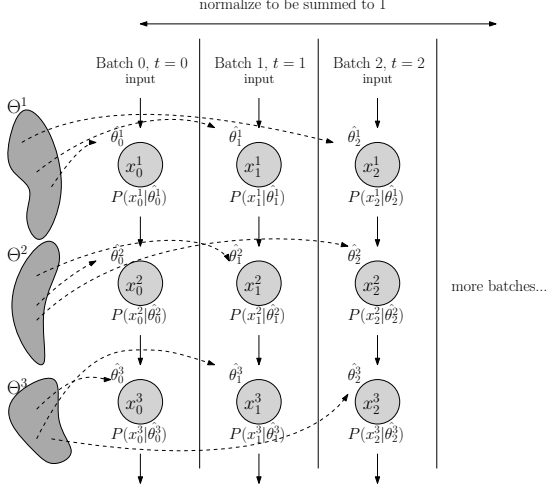


Figure 3: **Model selection in neural network.** If we consider each time step of the optimization (drawn here to be batch-dependent) as the process of choose the optimal model from model class Θ^i for i th layer of the neural networks, the optimized parameter $\hat{\theta}_j^i$ with subscript j as time step $t = j$ and superscript i as layer i can be assumed to be the optimal model among all models in the model class Θ^i . The normalized maximum likelihood can be computed by choosing $P(x_j^i | \hat{\theta}_j^i)$, the “optimal” model with shortest code length given data x_j^i , as the summing component in normalization.

ized by the parameter set θ . x_i are data sample from data X . With this distribution, the regret is the same for all data sample x given by [6]:

$$\begin{aligned} \text{COMP}(\Theta) &\equiv \text{regret}_{NML} \\ &\equiv -\log P_{NML}(x) + \log P(x|\hat{\theta}(x)) \\ &= \log \sum_{x'} P(x'|\hat{\theta}(x')) \end{aligned} \quad (2)$$

which defines the model class complexity as it indicates how many different data samples can be well explained by the model class Θ .

4 Neural networks as model selection

In the neural network setting where optimization process are performed in batches (as incremental data sample x_j with j denoting the batch j), the model selection process is formulated as a partially observable problem (as in Figure 3). Herein to illustrate our approach, we consider a feedforward neural network as an example, without loss of generalizability to other architecture (such as convolutional layers or recurrent modules). x_j^i refers to the activation at layer i at time point j (batch j). θ_j^i is the

parameters that describes x_j^i (i.e. weights for layer $i - 1$) optimized after $j - 1$ steps (seen batch 0 through $j - 1$). Because one cannot exhaust the search among all possible θ , we assume that the optimized parameter $\hat{\theta}_j^i$ at time step j (seen batch 0 through $j - 1$) is the optimal model $P(x_j^i | \hat{\theta}_j^i)$ for data sample x_j^i . Therefore, we generalize the optimal universal code with the NML formulation:

$$P_{NML}(x_i) = \frac{P(x_i | \hat{\theta}_i(x_i))}{\sum_{j=0}^i P(x_j | \hat{\theta}_j(x_j))} \quad (3)$$

where $\hat{\theta}_i(x_i)$ refers to the model parameter already optimized for $i - 1$ steps and have seen sequential data sample x_0 through x_{i-1} . This distribution is updated every time a new data sample is given, and can therefore be computed incrementally, as in batch-based training.

5 Unsupervised attention mechanism

5.1 Standard case: Regularity Normalization

We first introduce the standard formulation of UAM: the regularity normalization (RN). As outlined in Algorithm 1, the input would be the activation of each neurons in certain layer and batch. Parameters $COMP$ and θ are updated after each batch, through the incrementation in the normalization and optimization in the training respectively. As the numerator of P_{NML} at this step of normalization, the term $P(x_i | \hat{\theta}_t(x_i))$ is computed to be stored as a log probability of observing sample x_i in $N(\mu_{i-1}, \sigma_{i-1})$, the normal distribution with the mean and standard deviation of all past data sample history $(x_0, x_1, \dots, x_{i-1})$, with a Gaussian prior for $P(x|\hat{\theta}(x))$. The selection for the Gaussian prior is based on the assumption that each x is randomly sampled from a Gaussian distribution, and the parameter sets from model class Θ are Gaussian, while further research can explore other possible priors and inference methods for arbitrary priors.

As in Eq. 2, $COMP$ is the denominator of P_{NML} taken log, so the “increment” function takes in $COMP_t$ storing $\sum_{i=0}^{t-1} P(x_i | \hat{\theta}_i(x_i))$ and the latest batch of $P(x_t | \hat{\theta}_t(x_t))$ to be added in the denominator, stored as $COMP_{t+1}$. The “increment” step involves computing the log sum of two values, which can be numerically stabilized with the log-sum-exp trick². The normalization factor is then computed as the shortest code length L given the NML distribution, the universal code distribution in Eq. 3.

²In continuous data streams or time series analysis, the incrementation step can be replaced by integrating over the seen territory of the probability distribution X of the data.

5.2 Variant: Saliency Normalization

NML distribution can be modified to also include a data prior function, $s(x)$, given by [22]:

$$P_{NML}(x) = \frac{s(x)P(x|\hat{\theta}(x))}{\sum_{x'} s(x')P(x'|\hat{\theta}(x'))} \quad (4)$$

where the data prior function $s(x)$ can be anything, ranging from the emphasis of certain inputs, to the cost of certain data, or even top-down attention. For instance, we can introduce the prior knowledge of the fraction of labels (say, in an imbalanced data problem where the oracle informs the model of the distribution of each label in the training phase); or in a scenario where we wish the model to focus specifically on certain feature of the input, say certain texture or color (just like a convolution filter); or in the case where the definition of the regularity drifts (such as the user preferences over years): in all these possible applications, the normalization procedure can be more strategic given these additional information. Therefore, we formulate this additional functionality into our regularity normalization, to be saliency normalization (SN), where the P_{NML} is computed with the addition of a pre-specified data prior function $s(x)$.

5.3 Variant: beyond elementwise normalization

In our current setup, the normalization is computed elementwise, considering the implicit space of the model parameters to be one-dimensional (i.e. all activations across the batch and layer are considered to be represented by the same implicit space). Instead, the definition of the implicit can be more than one-dimensional to increase the expressibility of the method, and can also be user-defined. For instance, we can also perform the normalization over the dimension of the batch, such that each neuron in the layer should have an implicit space to compute the universal code. We term this variant regularity batch normalization (RBN). Similarly, we can perform regularity normalization over the layer dimension, as the regularity layer normalization (RLN). These two variants have the potential to inherit the innate advantages of batch normalization and layer normalization.

Algorithm 1 Regularity Normalization (RN)

Input: Values of x over a mini-batch: $\mathcal{B} = \{x_1, \dots, m\}$;

Parameter: $COMP_t, \hat{\theta}_t$

Output: $y_i = RN(x_i)$

$COMP_{t+1} = \text{increment}(COMP_t, P(x_i|\hat{\theta}_t(x_i)))$

$L_{x_i} = COMP_{t+1} - \log P(x_i|\hat{\theta}_t(x_i))$

$y_i = L_{x_i} * x_i$

6 Demo: UAM analysis for classification

In this section, we provide a demonstration (or tutorial) of how UAM can be applied to understand how unsupervised attention mechanism route relevant information during the learning process. We trained two types of deep networks on the simple image classification problem with the MNIST dataset [11]. In both experiments, training, validation and testing sets are shuffled into 55000, 5000, and 10000 cases. Batch size is set to 128. For optimization, stochastic gradient descent is used with learning rate 0.01 and momentum set to be 0.9. In both cases, we trained the task to mastery (over 97%) for vanilla FFNN and RNN over 10 epochs. We record the change of the minimum description length (computed incrementally from the optimal universal code in Eq. 3) of each layer over the entire training time (time stamped by batches).

6.1 Over different layers in FFNN

In this analysis, we consider the classical 784-1000-1000-10 feedforward neural network, two hidden layers with ReLU activation functions. We computed the minimum description length of each layer of the network (f_{c_1} and f_{c_2}) with respect to the last layer’s input.

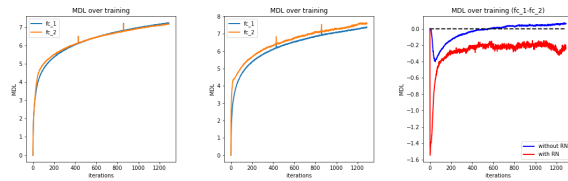


Figure 4: UAM in NN: MDL changes in a FFNN.

Figure 4 demonstrated the change of MDL over training time. We observe that the model complexities increases smoothly and then gradually converges to a plateau, matching the information bottleneck hypothesis of deep networks. The MDL for the later (or higher) layer seems to be having a higher model complexity in the start, but after around 600 iterations, the earlier (or lower) layer seems to catch up in the model complexities. Comparing the MDL curve of NN with or without the proposed regularity normalization, we observed that the regularization appeared to implicitly impose a constraint to yield a lower model complexity in earlier layers than later layers.

6.2 Over recurrent time steps in RNN

In this analysis, we consider a vanilla RNN with 100 hidden units over 5 time steps with tanh activation functions. We computed the minimum description length of each unfolded layer of the recurrent network (r_1 to r_5) with

respect to the last unfolded layer’s input. Similarly, we compare the UAM in two networks, one with the regularity normalization installed at each time step (or unfolded layer), and one without RN, i.e. the vanilla network.

Since an unfolded recurrent network can be considered equivalent to a deep feedforward network, in this analysis, we wish to understand the effect of regularity normalization on RNN’s layer-specific MDL beyond the effect on a simply deeper FFNN. We consider a recurrent unit to be also adapting to the statistical regularity not only over the training time dimension, but also the recurrent unfolded temporal dimension. In another word, we consider the recurrent units at different recurrent time step to be the same computing module at a different state in the model selection process (i.e. the same layer in Figure 3). Therefore, instead of keeping track of individual histories of the activations at each step, we only record one set of history for the entire recurrent history (by pooling all the activations from 0 to the current recurrent time steps).

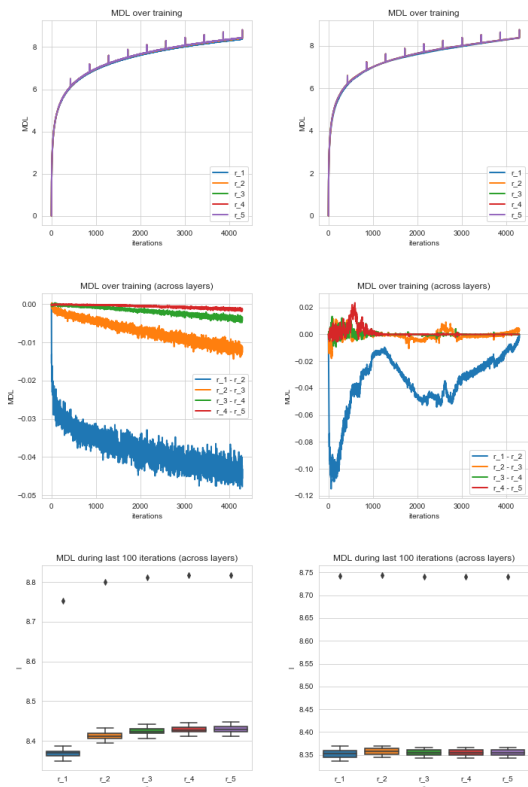


Figure 5: **UAM in RNN**: MDL changes in a 100-neuron RNN of 5 recurrent time steps with or without RN.

From Figure 5, we observe that both networks adopts a similar model complexity progression. Unlike traditional understanding of a asynchronous learning stages for different recurrent time steps, this analysis suggested that the

change of minimum description length during learning over different recurrent time steps are relatively universal. The model complexity of earlier time step (or earlier unfolded layer) seems to be much lower than later ones, and the margins are decreasing over the recurrent time step (Figure 5 middle and bottom row). In another word, a vanilla RNN appears to process the recurrent input in gradually increasing complexity until a plateau. As expected, the proposed regularity normalization regularizes the complexity assignments across recurrent time steps (as unfolded layers) such that the complexities of the later time steps remain a relatively low level. Further analysis on RNNs with different architectures, multiple layers and different activations functions can enlighten more insights on this kind of interesting behaviors.

7 Empirical results

7.1 Imbalanced MNIST problem with FFNN

As a proof of concept, we evaluated our approach on MNIST dataset [11] and computed the total number of classification errors as a performance metric. As we specifically wish to understand the behavior where the data inputs are non-stationary and highly imbalanced, we created an imbalanced MNIST benchmark to test seven methods: batch normalization (*BN*), layer normalization (*LN*), weight normalization (*WN*), and regularity normalization (*RN*), as well as three variants: saliency normalization (*SN*) with data prior as class distribution, regularity layer normalization (*RLN*) where the implicit space is defined to be layer-specific, and a combined approach where RN is applied after LN (*LN+RN*).

Given the nature of regularity normalization, it should better adapt to the regularity of the data distribution than other methods, tackling the imbalanced data issue by up-weighting the activation of the rare sample features and down-weighting those of the dominant features.

Experimental setting

To simulate changes in the context (input) distribution, in each epoch we randomly choose n classes out of the ten, and set their sampling probability to be 0.01 (only 1% of those n classes are used in the training). In this way, the training data may trick the models into preferring to classifying into the dominant classes. We built upon the classical 784-1000-1000-10 FFNN with ReLU activation functions for all six normalization methods, as well as the baseline neural network without normalization. As we are looking into the short-term sensitivity of the normalization method on the neural network training, one epoch of trainings are being recorded (all model face the same randomized imbalanced distribution). Training, valida-

Table 1: **Heavy-tailed scenarios:** test errors of the imbalanced permutation-invariant MNIST 784-1000-1000-10 task

	“Balanced”	“Rare minority”			“Highly imbalanced”			“Dominant oligarchy”		
	$n = 0$	$n = 1$	$n = 2$	$n = 3$	$n = 4$	$n = 5$	$n = 6$	$n = 7$	$n = 8$	$n = 9$
baseline	4.80 ± 0.15	14.48 ± 0.28	23.74 ± 0.28	32.80 ± 0.22	42.01 ± 0.45	51.99 ± 0.32	60.86 ± 0.19	70.81 ± 0.40	80.67 ± 0.36	90.12 ± 0.25
BN	2.77 ± 0.05	12.54 ± 0.30	21.77 ± 0.25	30.75 ± 0.30	40.67 ± 0.45	49.96 ± 0.46	59.08 ± 0.70	67.25 ± 0.54	76.55 ± 1.41	80.54 ± 2.38
LN	3.09 ± 0.11	8.78 ± 0.84	14.22 ± 0.65	20.62 ± 1.46	26.87 ± 0.97	34.23 ± 2.08	36.87 ± 0.64	41.73 ± 2.74	41.20 ± 1.13	41.26 ± 1.30
WN	4.96 ± 0.11	14.51 ± 0.44	23.72 ± 0.39	32.99 ± 0.28	41.95 ± 0.46	52.10 ± 0.30	60.97 ± 0.18	70.87 ± 0.39	80.76 ± 0.36	90.12 ± 0.25
RN	4.91 ± 0.39	8.61 ± 0.86	14.61 ± 0.58	19.49 ± 0.45	23.35 ± 1.22	33.84 ± 1.69	41.47 ± 1.91	60.46 ± 2.88	81.96 ± 0.59	90.11 ± 0.24
RLN	5.01 ± 0.29	9.47 ± 1.21	12.32 ± 0.56	22.17 ± 0.94	23.76 ± 1.56	32.23 ± 1.66	43.06 ± 3.56	57.30 ± 6.33	88.36 ± 1.77	89.55 ± 0.32
LN+RN	4.59 ± 0.29	8.41 ± 1.16	12.46 ± 0.87	17.25 ± 1.47	25.65 ± 1.91	28.71 ± 1.97	33.14 ± 2.49	36.08 ± 2.09	44.54 ± 1.74	82.29 ± 4.44
SN	7.00 ± 0.18	12.27 ± 1.30	16.12 ± 1.39	24.91 ± 1.61	31.07 ± 1.41	41.87 ± 1.78	52.88 ± 2.09	68.44 ± 1.42	83.34 ± 1.85	82.41 ± 2.30

tion and testing sets are shuffled into 55000, 5000, and 10000 cases. In the testing phase, the data distribution is restored to be balanced, and no models have access to the other testing cases or the data distribution. Batch size is set to 128. Stochastic gradient descent is used with learning rate 0.01 and momentum set to be 0.9.

The imbalanced degree n is defined as following: when $n = 0$, it means that no classes are downweighted, so we termed it the “*fully balanced*” scenario; when $n = 1$ to 3, it means that a few cases are extremely rare, so we termed it the “*rare minority*” scenario. When $n = 4$ to 8, it means that the multi-class distribution are very different, so we termed it the “*highly imbalanced*” scenario; when $n = 9$, it means that there is one or two dominant classes that is 100 times more prevalent than the other classes, so we termed it the “*dominant oligarchy*” scenario. In real life, *rare minority* and *highly imbalanced* scenarios are very common, such as predicting the clinical outcomes of a patient when the therapeutic prognosis data are mostly tested on one gender versus the others, or in reinforcement learning setting where certain or most types of rewards are very sparse and non-stationary across episodes.

Performance

Table 1 reports the test errors (in %) with their standard errors of eight methods in 10 training conditions over two heavy-tailed scenarios: labels with under-represented and over-represented minorities. In the balanced scenario, the proposed regularity-based method doesn’t show clear advantages over existing methods, but still managed to perform the classification tasks without major deficits. In both the “rare minority” and “highly imbalanced” scenarios, regularity-based methods performs the best in all groups, suggesting that the proposed method successfully constrained the model to allocate learning resources to the “special cases” which are rare and out of normal range, while BN and WN failed to learn it completely (as in the confusion matrices in Appendix B). In the “dominant oligarchy” scenario, LN performs the best, dwarfing all other normalization methods. However, as in the case of $n = 8$, LN+RN performs considerably well, with performance within error bounds to that of LN, beating other normalization methods by over 30 %. It is noted

that LN also managed to capture the features of the rare classes reasonably well in other imbalanced scenarios, comparing to BN, WN and baseline. The hybrid methods RLN and LN+RN both displays excellent performance in the imbalanced scenarios, suggesting that combining regularity-based normalization with other methods is advantageous, as the regularization priors they each impose are in different dimensions and subspaces.

The results presented here mainly dealt with the short term domain to demonstrate how regularity can significantly speed up the training. The long term behaviors tend to converge to a balanced scenario since the regularities of the features and activations will become higher (not rare anymore), with the normalization factors converging to a constant. As a side note, despite the significant margin of the empirical advantages, we observe that regularity-based approach offers a larger standard deviation in the performance than the baselines. We suspected the following reason: the short-term imbalanceness should cause the normalization factors to be considerably distinct across runs and batches, with the rare signals amplified and common signals tuned down; thus, we expect that the predictions to be more extreme (the wrong more wrong, the right more right), i.e. a more stochastic performance by individual, but a better performance by average. We observed this effect to be smaller in the long term (when normalization factors converge to a constant). Further analysis need to be included to fully understand these behaviors in different time scales (e.g. the converging performance over 100 epochs). Test accuracy results in the highly imbalanced scenario (RN over BN/WN/baseline for around 20%) should provide promises in its ability to learn from the extreme regularities.

Dissecting UAM

Figure 6 demonstrated three stereotypical MDL curves in the three imbalanced scenarios. In all three cases, the later (or higher) layer of the FFNN adopts a higher model complexity. The additional regularity normalization seems to drive the later layer to accommodate for the additional model complexities due to the imbalanced nature of the dataset, and at the same time, constraining the low-level representations (earlier layer) to have a smaller descrip-

tion length in the implicit space. This behaviors matches our hypothesis how this type of regularity-based normalization can extract more relevant information in the earlier layers as inputs to the later ones, such that later layers can accommodate a higher complexity for subsequent tasks.

Figure 7 compared the effect of imbalanceness on the MDL difference of the two layers in NN with or without RN. We observed that when the imbalanceness is higher (i.e. n is smaller), a vanilla NN tends to maintains a significant complexity difference for more iterations before converging to a similar levels of model complexities between layers. On the other hand, RN constrained the imbalanceness effect with a more consistent level of complexity difference, suggesting a possible link of this stable complexity difference with a robust performance in the imbalanced scenarios (as RN demonstrated).

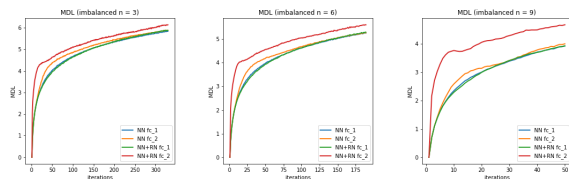


Figure 6: MDL changes in imbalanced MNIST.

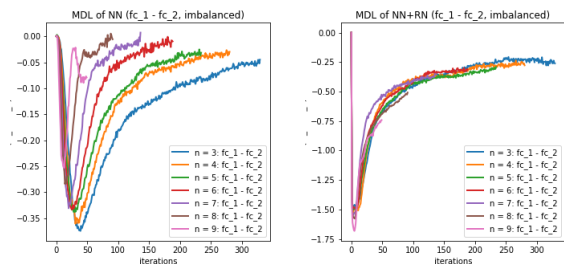


Figure 7: Layer trade-off in various imbalanceness.

7.2 Reinforcement learning problem with DQN

We further evaluated the benefit of the proposed approach in the game setting of the reinforcement learning problem, where the rewards can be sparse. For simplicity, we consider the classical deep Q network [14] and tested it in OpenAI Gym’s LunarLander and CarPole environments [3] (see Appendix A.1 for game setting). Five agents (DQN, DQN+LN, DQN+RN, DQN+RLN, DQN+RN+LN) are being considered and evaluated by the final scores over 2000 episodes across 50 runs.

Experimental setting

The Q networks consist of with two hidden layers of 64 neurons. With experience replay [13], the learning of the

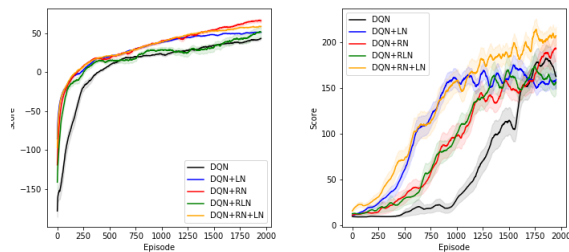


Figure 8: Scores in LunarLander (L) and CarPole (R).

DQN agents was implemented as Actor-Critic algorithm [10] with the discount factor $\gamma = 0.99$, the soft update rate $\tau = 0.001$, the learning rate $lr = 0.001$, epsilon greedy exploration from 1.0 to 0.01 with decay rate of 0.95, the buffer size 10,000, the batch size 50 and optimization algorithm Adam [9]. To adopt the proposed incremental MDL normalization method, we installed the normalization to both the local and target Q networks.

Performance

Figure 8 demonstrated the learning curves of the five competing agents over 2000 episodes of learning with their standard errors over 50 runs. Evaluating by the averaged final scores in LunarLander, DQN+RN (66.27 ± 2.45) performs the best among all five agents, followed by DQN+RN+LN (58.90 ± 1.10) and DQN+RLN (51.50 ± 6.58). All three proposed agents beat DQN (43.44 ± 1.33) and DQN+LN (51.49 ± 0.57) by a large marginal. The learning curve also suggested that taking regularity into account speed up the learning and helped the agents to converge much faster than the baseline.

Similarly in CarPole, DQN+RN+LN (206.99 ± 10.04) performs the best among all five agents, followed by DQN+RN (193.12 ± 14.05), beating DQN (162.77 ± 13.78) and DQN+LN (159.08 ± 8.40) by a large marginal. These numerical results suggested the proposed method has the potential to benefit the neural network training in reinforcement learning setting. On the other hand, certain aspects of these behaviors are worth further exploring. For example, the proposed methods with highest final scores do not converge as fast as DQN+LN, suggesting that regularity normalization resembles some type of adaptive learning rate which gradually tune down the learning as scenario converges to stationarity.

Dissecting UAM

As shown in Figure 9, the DQN has a similar MDL change during the learning process to the ones in the computer vision task. We observe that the MDL curves are more separable when regularity normalization is installed. This suggested that the additional RN constrained the earlier

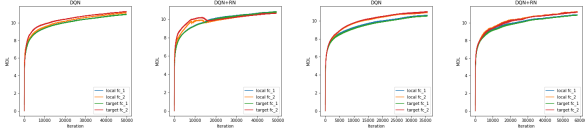


Figure 9: **MDL changes** in the local and target Q networks in a two-layer DQN with or without RN in LunarLander (left two) and CarPole (right two).

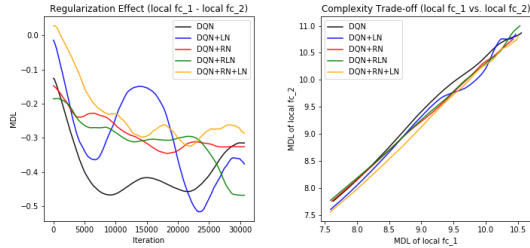


Figure 10: **Layer trade-off** in local networks (CarPole).

(or lower) layer to have a lower complexity in the implicit space and saving more complexities into higher layer. The DQN without RN, on the other hand, has a more similar layer 1 and 2. We also observe that the model complexities (by the MDL) of the target networks seems to be more diverged in DQN comparing with the DQN+RN, suggesting the RN as a advantageous regularization for the convergence of the local to the target networks. Figure 10 offered some intuition why this is the case: the RN (red curve) seems to maintain the most stable complexity difference between layers, which stabilizes the learning and provides a empirically advantages trade-off among the expressiveness of layers given a task (see Appendix A.2 for a complete spectrum of this UAM analysis).

8 Discussion

Empirical results offered a proof of concept to the proposed unsupervised attention mechanism. In the tasks of the image classification and the reinforcement learning problem, our approach empirically outperforms existing normalization methods in the imbalanced, limited, or non-stationary data scenario as hypothesized. However, several analyses and developments are worth pursuing to further understanding of the behaviors.

First, the metric use in the MNIST problem is the test error (as usually used in the normal case comparison). Although the proposed method is shown to have successfully constrained the model to allocate learning resources to the several imbalanced special cases, there might exist better performance metric specially tailored for these special cases. Second, the probability inference can be replaced

with a fully Bayesian variational inference approach to include the regularity estimation as part of the optimization. Moreover, although the results shows the proposed regularity-based normalization has an improvement on MNIST, it would be additionally interesting to record the overall loss or probability as the computation of NML makes selection on the model, like a partially observable routing process of representation selection as in [12].

Last but not least, in traditional model selection problems, MDL can be regarded as ensemble modeling process and usually involves multiple models. However, in our neural network problem, we assume that the only model trained at each step is the local “best” model learned so far, i.e. a partially observable model selection problem. This implies that the local maximal likelihood may not be a global best solution for model combinations, because the generation of optimized parameter set for a specific layer currently adopts greedy approach, such that the model selection could be optimized for each step. Further theoretical work is worth pursuing to demonstrate whether this greedy approach converges to the best global selection.

9 Conclusion and Future Work

Inspired by the neural code adaptation of biological brains, we propose a biologically plausible unsupervised attention mechanism taking into account the regularity of the activation distribution in the implicit space, and normalize it to upweight activation for rarely seen scenario and downweight activation for commonly seen ones. We proposed to consider neural network training process as a model selection problem and computed the model complexity of a neural network layer as the optimal universal code length by normalized maximum likelihood. We showed that this code length can serve as a normalization factor and can be easily incorporated with established regularization methods to (1) speed up training, (2) increase the sensitivity to imbalanced data or feature spaces, and (3) analyze and understand neural networks in action via the lens of model complexity.

One main next direction of this research is the top-down attention given by data prior (such as feature extracted from signal processing, or task-dependent information). For instance, the application of top-down attention $s(x)$ to modulate the normalization process can vary in different scenarios. Further investigation of how different functions of $s(x)$ behave in different task settings may complete the story of having this method as a top-down meta learning algorithm potentially advantageous for continual multitask learning. Imposed on the input data and layer-specific activations, unsupervised attention mechanism has the flexibility to directly install top-down attention from either oracle supervision or other meta information.

References

- [1] Jimmy Lei Ba, Jamie Ryan Kiros, and Geoffrey E Hinton. Layer normalization. *arXiv preprint arXiv:1607.06450*, 2016.
- [2] C_ Blakemore and Fergus W Campbell. Adaptation to spatial stimuli. *The Journal of physiology*, 200(1):11P–13P, 1969.
- [3] Greg Brockman, Vicki Cheung, Ludwig Pettersson, Jonas Schneider, John Schulman, Jie Tang, and Wojciech Zaremba. Openai gym. *arXiv preprint arXiv:1606.01540*, 2016.
- [4] Stephanie Ding, Christopher J Cueva, Misha Tsodyks, and Ning Qian. Visual perception as retrospective bayesian decoding from high-to low-level features. *Proceedings of the National Academy of Sciences*, 114(43):E9115–E9124, 2017.
- [5] Valentin Dragoi, Jitendra Sharma, and Mriganka Sur. Adaptation-induced plasticity of orientation tuning in adult visual cortex. *Neuron*, 28(1):287–298, 2000.
- [6] Peter D Grünwald. *The minimum description length principle*. MIT press, 2007.
- [7] Geoffrey Hinton and Drew Van Camp. Keeping neural networks simple by minimizing the description length of the weights. In *in Proc. of the 6th Ann. ACM Conf. on Computational Learning Theory*. Citeseer, 1993.
- [8] Sergey Ioffe and Christian Szegedy. Batch normalization: Accelerating deep network training by reducing internal covariate shift. *arXiv preprint arXiv:1502.03167*, 2015.
- [9] Diederik P Kingma and Jimmy Ba. Adam: A method for stochastic optimization. *arXiv preprint arXiv:1412.6980*, 2014.
- [10] Vijay R Konda and John N Tsitsiklis. Actor-critic algorithms. In *Advances in neural information processing systems*, pages 1008–1014, 2000.
- [11] Yann LeCun. The mnist database of handwritten digits. <http://yann.lecun.com/exdb/mnist/>, 1998.
- [12] Baihan Lin, Djallel Bouneffouf, Guillermo A Cecchi, and Irina Rish. Contextual bandit with adaptive feature extraction. In *2018 IEEE International Conference on Data Mining Workshops (ICDMW)*, pages 937–944. IEEE, 2018.
- [13] Long-Ji Lin. Self-improving reactive agents based on reinforcement learning, planning and teaching. *Machine learning*, 8(3-4):293–321, 1992.
- [14] Volodymyr Mnih, Koray Kavukcuoglu, David Silver, Alex Graves, Ioannis Antonoglou, Daan Wierstra, and Martin Riedmiller. Playing atari with deep reinforcement learning. *arXiv preprint arXiv:1312.5602*, 2013.
- [15] Jay I Myung, Daniel J Navarro, and Mark A Pitt. Model selection by normalized maximum likelihood. *Journal of Mathematical Psychology*, 50(2):167–179, 2006.
- [16] Ning Qian and Jun Zhang. Neuronal firing rate as code length: a hypothesis. *Computational Brain & Behavior*, pages 1–20, 2019.
- [17] Jorma Rissanen. Modeling by shortest data description. *Automatica*, 14(5):465–471, 1978.
- [18] Jorma Rissanen. *Stochastic complexity in statistical inquiry*. World Scientific, 1989.
- [19] Jorma Rissanen. Strong optimality of the normalized ml models as universal codes and information in data. *IEEE Transactions on Information Theory*, 47(5):1712–1717, 2001.
- [20] Tim Salimans and Durk P Kingma. Weight normalization: A simple reparameterization to accelerate training of deep neural networks. In *Advances in Neural Information Processing Systems*, pages 901–909, 2016.
- [21] Richard S Zemel and Geoffrey E Hinton. Learning population coes by minimizing description length. In *Unsupervised learning*, pages 261–276. Bradford Company, 1999.
- [22] Jun Zhang. Model selection with informative normalized maximum likelihood: Data prior and model prior. In *Descriptive and normative approaches to human behavior*, pages 303–319. World Scientific, 2012.

A Supplementary Information for Reinforcement Learning Tasks

A.1 Game Setting

In LunarLander, the agent learns to land on the exact coordinates of the landing pad (0,0) during a free fall motion starting from zero speed to the land with around 100 to 140 actions, with rewards fully dependent on the location of the lander (as the state vector) on the screen in a non-stationary fashion: moving away from landing pad loses reward; crashes yields -100; resting on the ground yields +100; each leg ground contact yields +10; firing main engine costs -0.3 points each frame; fuel is infinite. Four discrete actions are available: do nothing, fire left orientation engine, fire main engine, fire right orientation engine.

In CarPole, the agent learns to control a pole attached by an un-actuated joint to a cart, which moves along a frictionless track, such that it doesn't fall over. The episode ends when the pole is more than 15 degrees from vertical, or the cart moves more than 2.4 units from the center and a reward of +1 is provided for every timestep that the pole remains upright. Two discrete actions are available: applying a force of +1 or -1 to the cart to make it go left or go right.

A.2 Supplementary Figures

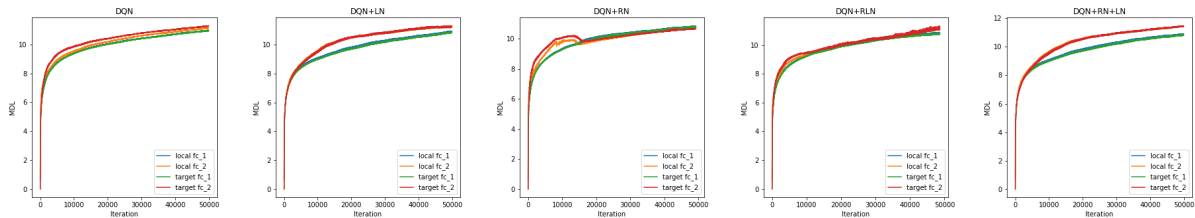


Figure 11: LunarLander: MDL changes in the local and target Q networks in DQN with different regularizations.

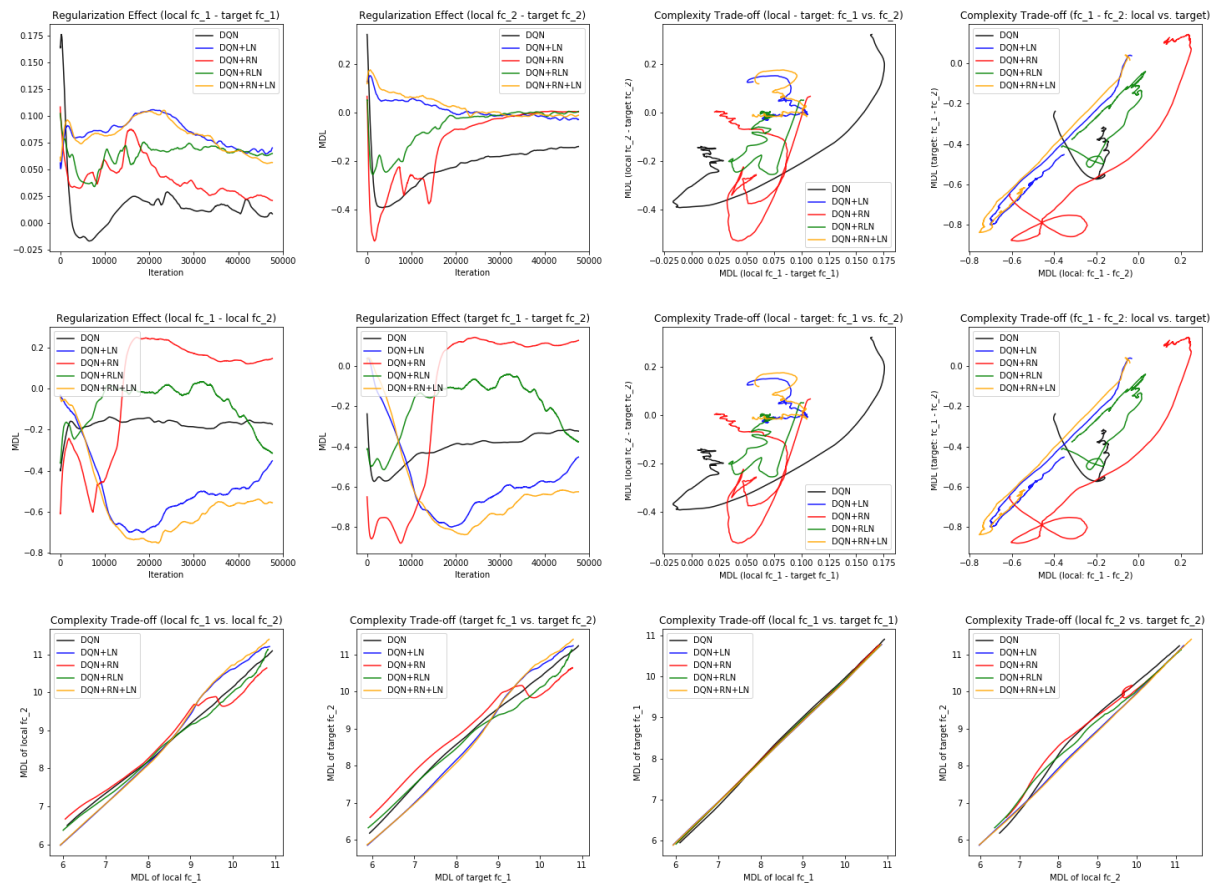


Figure 12: LunarLander: visualizations of regularization effects on the model complexities.

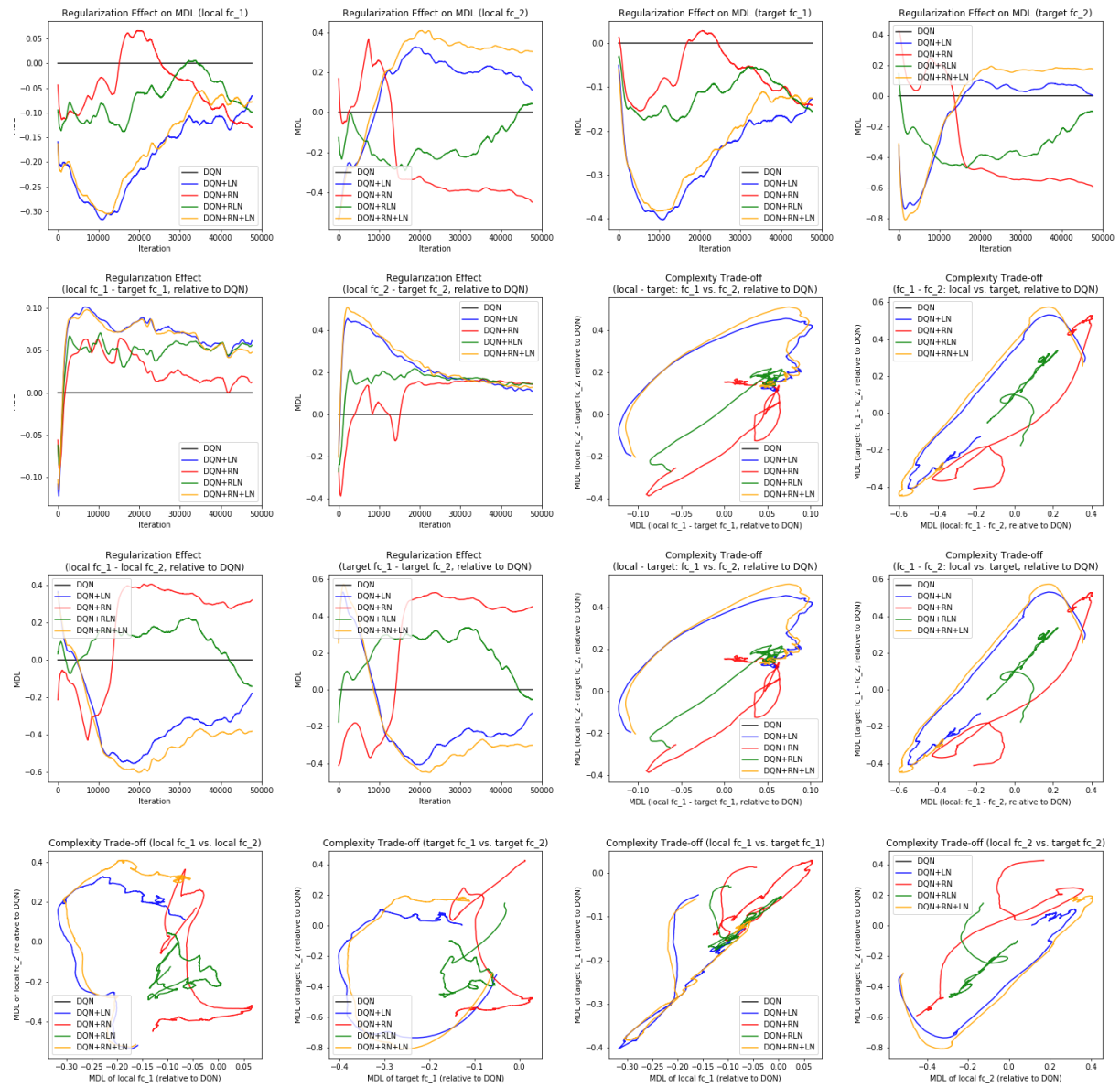


Figure 13: LunarLander: visualizations of regularization effects on the model complexities, plotted relative to DQN.

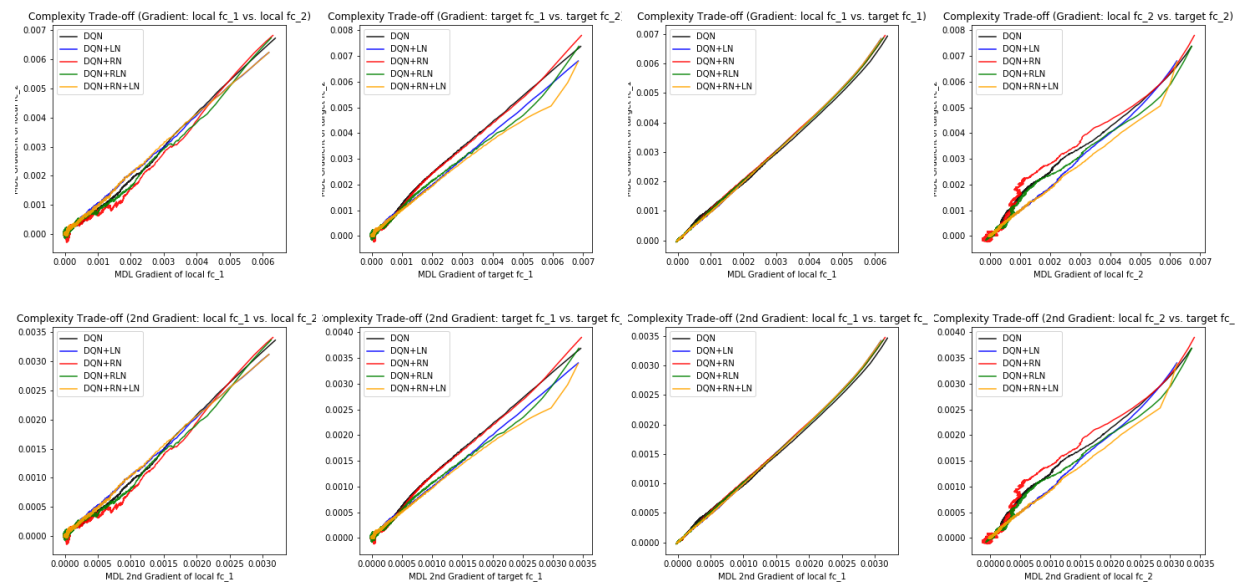


Figure 14: LunarLander: visualizations of 1st and 2nd-order derivative of MDL with respect to training iterations.

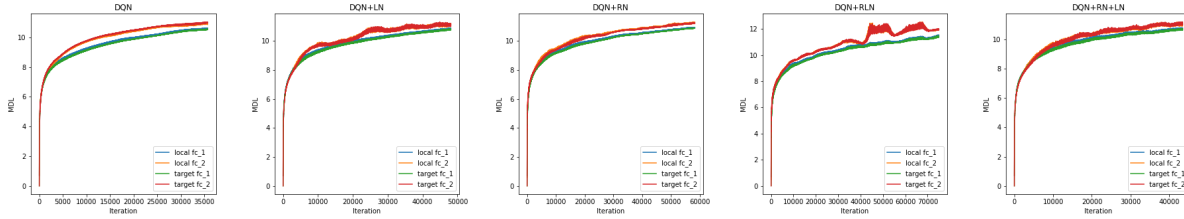


Figure 15: **CarPole**: MDL changes in the local and target Q networks in DQN with different regularizations.

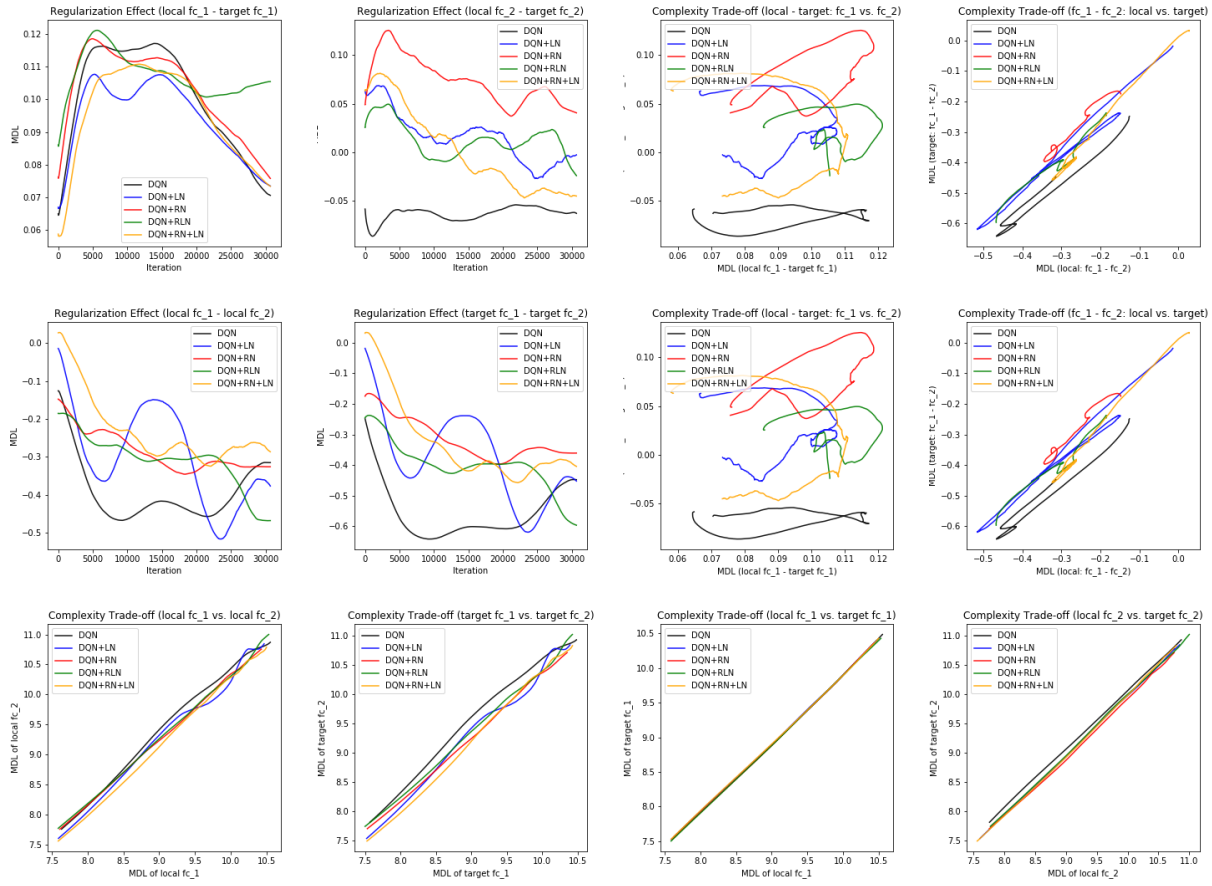


Figure 16: **CarPole**: visualizations of regularization effects on the model complexities.

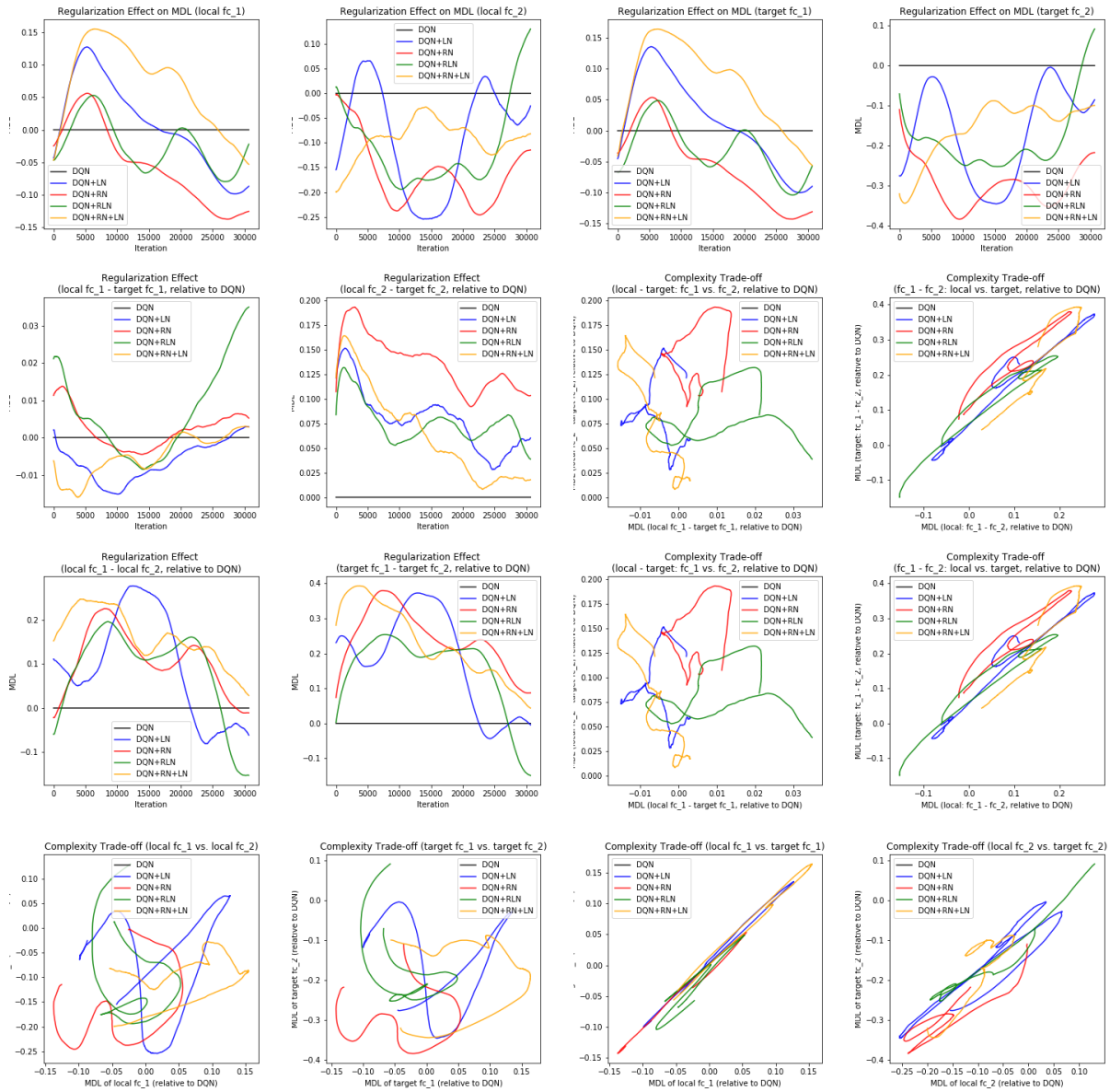


Figure 17: **CarPole**: visualizations of regularization effects on the model complexities, plotted relative to DQN.

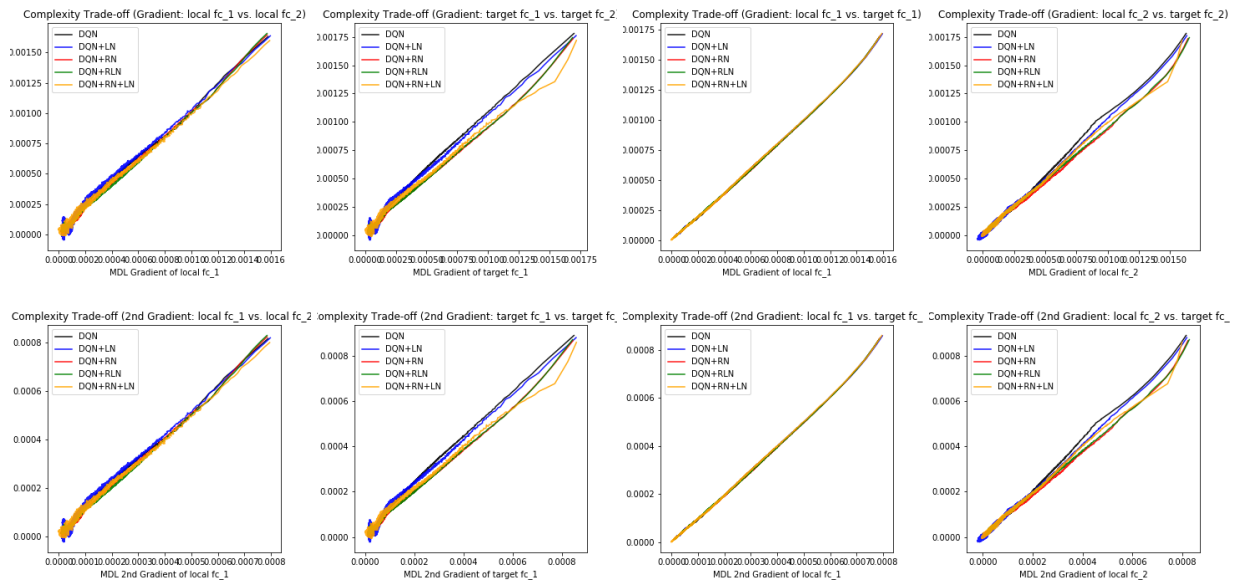


Figure 18: **CarPole**: visualizations of 1st and 2nd-order derivative of MDL with respect to training iterations.

B Supplementary Figures for Imbalanced MNIST Tasks



Figure 19: **Confusion matrices** of imbalanced MNIST in the short-term: rows are scenarios ($n=0, 1, 2, 3, 4, 5, 6, 7, 8, 9$) and columns are algorithms (baseline, BN, LN, WN, RN, RLN, LN+RN, SN).